Contents lists available at ScienceDirect

Biochemistry and Biophysics Reports

The protective effect of astaxanthin on the ganglion cell complex in glutamate/aspartate transporter deficient mice, a model of normal tension glaucoma, analyzed by spectral domain-optical coherence tomography

Takayuki Tanaka-Gonome, Yuting Xie, Kodai Yamauchi, Natsuki Maeda-Monai, Reiko Tanabu, Takashi Kudo, Mitsuru Nakazawa *

Department of Ophthalmology, Hirosaki University Graduate School of Medicine, Hirosaki, 036-8562, Japan

ARTICLE INFO

ABSTRACT

Astaxanthin (AST), a natural marine carotenoid, possess a wide variety of biological functions. In particular, as a strong antioxidant, AST effectively scavenges oxygen free radicals and reduces oxidative stress. In addition, recent *in vitro* studies have suggested that AST attenuates glutamate-induced apoptosis and cytotoxicity. The glutamate/aspartate transporter (GLAST) deficient (GLAST$^{-/-}$) mouse is a mouse model of normal tension glaucoma (NTG) caused by both the glutamate neurotoxicity and oxidative stress in the retina. In the present study, we investigated the effects of AST on the ganglion cell complex, indicator of glaucomatous structural damage, using spectral domain-optical coherence tomography. As a result, AST significantly attenuated the thinning of ganglion cell complex in GLAST$^{-/-}$ mice in comparison to an AST-free control group. Our results suggest the possibility that AST has protective effects against glutamate neurotoxicity and oxidative stress in the retina. At present, the only treatment for NTG that is available in the clinical setting is to reduce the IOP as much as possible. Thus, our results suggest that AST supplementation may be effective for some types of NTG in which glutamate neurotoxicity and oxidative stress are involved.

1. Introduction

Glaucoma, one of the leading causes of blindness worldwide, is characterized by the progressive degeneration of retinal ganglion cells (RGCs). It causes irreversible visual field loss and optic nerve degeneration. While it is usually associated with elevated intraocular pressure (IOP), there is a subtype of glaucoma termed normal tension glaucoma (NTG) in which an affected individual presents an IOP within a statistically normal range. Although no obvious causes of NTG have been identified, the optic nerve becomes susceptible to damage, even at the normal range of IOP in NTG. In addition to IOP, the following factors have been proposed as possible causes: impaired ocular blood flow, genetic factors, aging, oxidative stress, glutamate neurotoxicity, myopia and reduced neurotrophic factors [1–8]. Since little is known about why the normal range of IOP causes damage in NTG, at present, the only treatment strategy available in the clinical setting is to reduce the IOP as much as possible.

The glutamate/aspartate transporter (GLAST)-deficient (GLAST$^{-/-}$)

mouse is used as a model of NTG because it demonstrates the progressive loss of RGCs and optic nerve degeneration without an elevated IOP. The reason for the loss of RGCs and optic nerve degeneration in the GLAST$^{-/-}$ mice has been thought to be glutamate neurotoxicity and oxidative stress [9]. Glutamate is one of the major excitatory neurotransmitters in the mammalian retina, and is integrated from the extracellular space via glutamate transporter. GLAST is expressed in Müller cells, and it incorporates glutamate released by synaptic signaling in the retinal extracellular space [10]. This system contributes to glutamate homeostasis in the retina. Thus, impaired GLAST leads to the accumulation of extracellular glutamate, which causes glutamate neurotoxicity in the retina. Moreover, the uptake of glutamate by GLAST into the Müller cells provides a substrate for synthesizing glutathione, which is an important radical scavenger [11]. Glutathione, as an antioxidant, has a strong protective role against oxidative stress in the retina [12]. Therefore, the GLAST expressed in Müller cells is essential not only for keeping the extracellular glutamate concentration below the neurotoxic level, but also for maintaining the glutathione levels in the retina by providing the
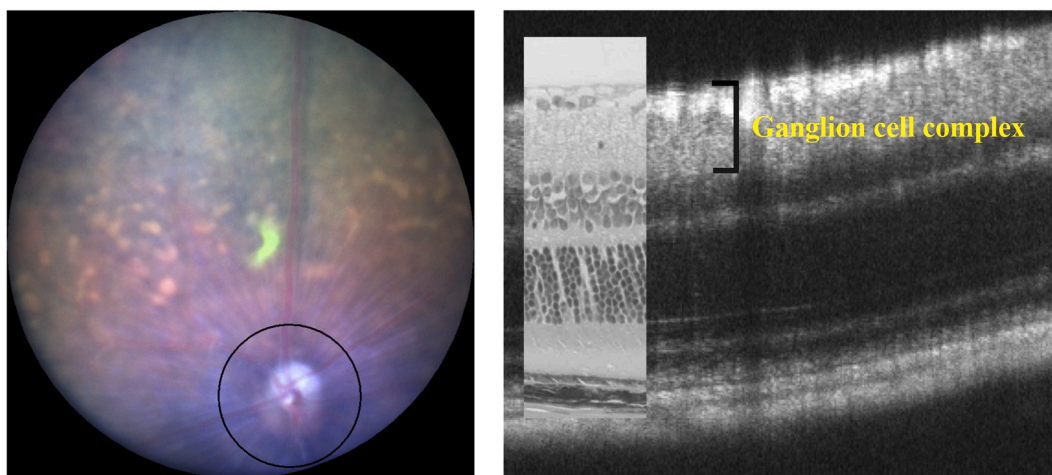
Fig. 1. Methods of SD-OCT examination by Micron® IV, and the relationship between the SD-OCT (P106) image findings and the histological findings in hematoxylin and eosin-stained sections (P120) of the C57BL/6J mouse retina.

substrate for glutathione synthesis.

Astaxanthin (AST, 3,3′-dihydroxy-β,β-carotene-4,4′-dione), a natural marine carotenoid, is found in many kinds of marine organisms, including salmon trout, shrimp, lobster, and fish eggs [13]. AST has been reported to possess a wide variety of biological functions, including anti-inflammatory, anti-carcinogenic and anti-diabetic activities, as well as neuroprotective effects in both *in vivo* and *in vitro* studies [13–15]. In particular, as a strong antioxidant, AST effectively scavenges oxygen free radicals and reduces oxidative stress [13]. Furthermore, recent studies showed that AST attenuated glutamate-induced apoptosis and cytotoxicity in *in vitro* studies. Wen et al. reported that AST significantly attenuated glutamate-induced cell viability loss by attenuating caspase activation, mitochondrial dysfunction and modulating Akt/GSK-3β signaling in HT22 cells, a mouse hippocampal neuronal cell line, after exposure to glutamate [16]. Moreover, Lin et al. reported that AST might attenuate glutamate-induced apoptotic signals via suppression of reactive oxygen species production and calcium influx, thus leading to the alleviation of endoplasmic reticulum stress and the modulation of Bcl-2 family proteins in SH-SY5Y cells, a human neuroblastoma cell line, after exposure to glutamate [17]. In addition, it has been reported that AST also has protective effects in the retina [18–20].

Thus, in the present study, we evaluated the effects of AST on thinning of the ganglion cell complex (GCC) in GLAST$^{-/-}$ mice using spectral-domain optical coherence tomography (SD-OCT). The GCC is three-layered structure consisting of a layer of retinal nerve fiber, a layer of retinal ganglion cell, and an inner plexiform layer, which is an indicator of glaucomatous structural damage. We have suspected that AST has a protective effect on the GCC in GLAST$^{-/-}$ mice. In addition, we investigated the morphological changes by electron microscopy.

2. Materials and methods

2.1. Experimental animals

All experimental procedures performed in this study conformed to the regulations of the Association for Research in Vision and Ophthalmology (ARVO) Statement for the Use of Animals in Ophthalmic and Vision Research and were approved by the institutional committee on ethics for animal experiments (Approval Number: M18019).

GLAST$^{-/-}$ mice were generously provided by Dr. Takayuki Harada (Visual Research Project, Tokyo Metropolitan Institute of Medical Science, Tokyo, Japan) [21]. C57BL/6J mice were purchased from Clea, Japan (Tokyo, Japan) and were used as wild-type controls. The mice were kept in the Hirosaki University Graduate School of Medicine Animal Care Service Facility under a cycle of 12-h of light (50 lx

illumination) and 12 h of darkness (<10 lx environmental illumination) in an air-conditioned atmosphere. Mice were given *ad libitum* access to food and water. The AST group was fed a diet containing 0.1% AST. AST powder was generously provided by AstaReal (Tokyo, Japan) and mixed with Oriental MF supplied by Oriental Food (Tokyo, Japan). Control groups were fed with Oriental MF alone. AST was mixed with oriental MF powder (Oriental Food) so that the final concentration of AST became 0.1%. Since carotenoids such as AST are known to be transferred to the fetus and breast milk, the feeding was started from prenatal pregnancy [22,23]. The results of GLAST$^{-/-}$ mice and C57BL/6J mice fed Oriental MF alone have been previously reported [24,25].

2.2. SD-OCT examination

SD-OCT were performed according to previously described methods using a Micron® IV (Phoenix Research Labs, Pleasanton, CA, USA) [24]. In brief, SD-OCT was carried out at 4 time points from postnatal (P) day 44 to P156 (P44, P80, P114 and P156) for control fed GLAST$^{-/-}$ mice, at 4 time points from P50 to P157 (P50, P78, P106 and P150) for GLAST$^{-/-}$ mice fed with AST containing food (+AST), and at 4 time points from P36 to P148 (P36, P72, P106 and P148) for C57BL/6J mice. The mice were anesthetized with an intraperitoneal injection of a mixture of medetomidine hydrochloride (0.315 mg/kg), midazolam (2.0 mg/kg), and butorphanol tartrate (2.5 mg/kg). The pupils were dilated with the instillation of eye drops containing a mixture of 0.5% tropicamide and 0.5% phenylephrine hydrochloride. The mouse ocular fundus was simultaneously monitored by a fundus camera, and the position of the retinal SD-OCT image was set circumferentially around the optic disc by considering potential structural differences between the upper and lower hemispheres of the mouse eye (360°; diameter, 500 μm; 140 μm away from the optic disc margin; Fig. 1) [24,25]. The corneal surface was protected using a 1.5% hydroxyethyl cellulose solution. Fifty images were averaged to eliminate projection artifacts. The quantitative analysis of the acquired SD-OCT images was performed using the InSight® software program (Phoenix Research Labs). During all experimental procedures, the physical condition of the mice was frequently monitored by inspection and gentle palpation by the researchers.

2.3. Measurement of the ganglion cell complex thickness

We measured the thickness of the GCC. Segmentation was performed using the InSight® software program, as previously reported [24,25]. The borderlines of the GCC sublayer were automatically identified by the software program using SD-OCT images and were manually corrected by the researchers when necessary. The average distance (μm) of
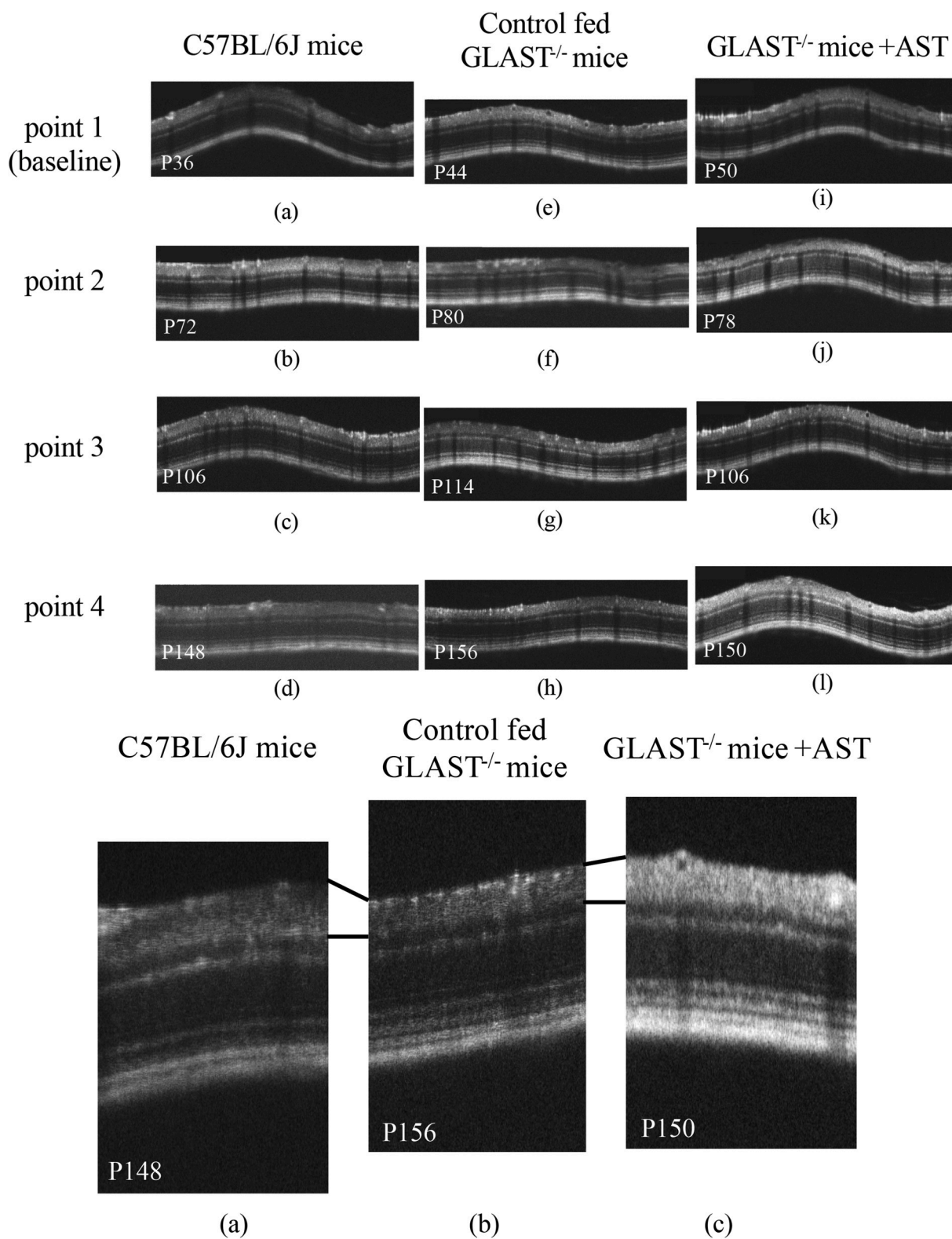
Fig. 2. A (the uppermost panel). Representative SD-OCT images of C57BL/6J mice (a, b, c, and d), control fed GLAST$^{-/-}$ mice (e, f, g, and h), and GLAST$^{-/-}$ mice + AST (i, j, k, and l). Panels a, b, c, and d correspond to C57BL/6J mice at P36, P72, P106, and P148, respectively. Panels e, f, g, and h correspond to control fed GLAST$^{-/-}$ mice at P44, P80, P114, and P156, respectively. Panels i, j, k, and l correspond to GLAST$^{-/-}$ mice + AST at P50, P78, P106, and P150, respectively.
B (the second upper panel). Comparison of the GCC thickness at the final observation point observed by SD-OCT in C57BL/6J mice (a), control fed GLAST$^{-/-}$ mice (b), and GLAST$^{-/-}$ mice + AST (c).
C (the third upper panel). The longitudinal changes in the thickness of the GCC. Diamonds, C57BL/6J mice; closed circles, control fed GLAST$^{-/-}$ mice; open circles, GLAST$^{-/-}$ mice + AST. Animal numbers: C57BL6J mice, P36~P148 (n = 4); control fed GLAST$^{-/-}$, P44~P114 (n = 4), p156 (n = 5); GLAST$^{-/-}$ mice + AST, P50 (n = 6), P78~P106 (n = 5), P150 (n = 4). Statistical significance: ***, P < 0.001 (Student's t-test). Bars indicate standard error

D (the bottom panel). Comparison of the change in the GCC thickness from the baseline to each observation points. Diamonds, C57BL/6J mice; closed circles, control fed GLAST$^{-/-}$ mice; open circles, GLAST$^{-/-}$ mice + AST. Animal numbers: C57BL6J mice, P36~P148 (n = 4); control fed GLAST$^{-/-}$, P44~P114 (n = 4), p156 (n = 5); GLAST$^{-/-}$ mice + AST, P50 (n = 6), P78~P106 (n = 5), P150 (n = 4). Statistical significance: *, $P < 0.05$ (Student's t-test). Bars indicate standard error.
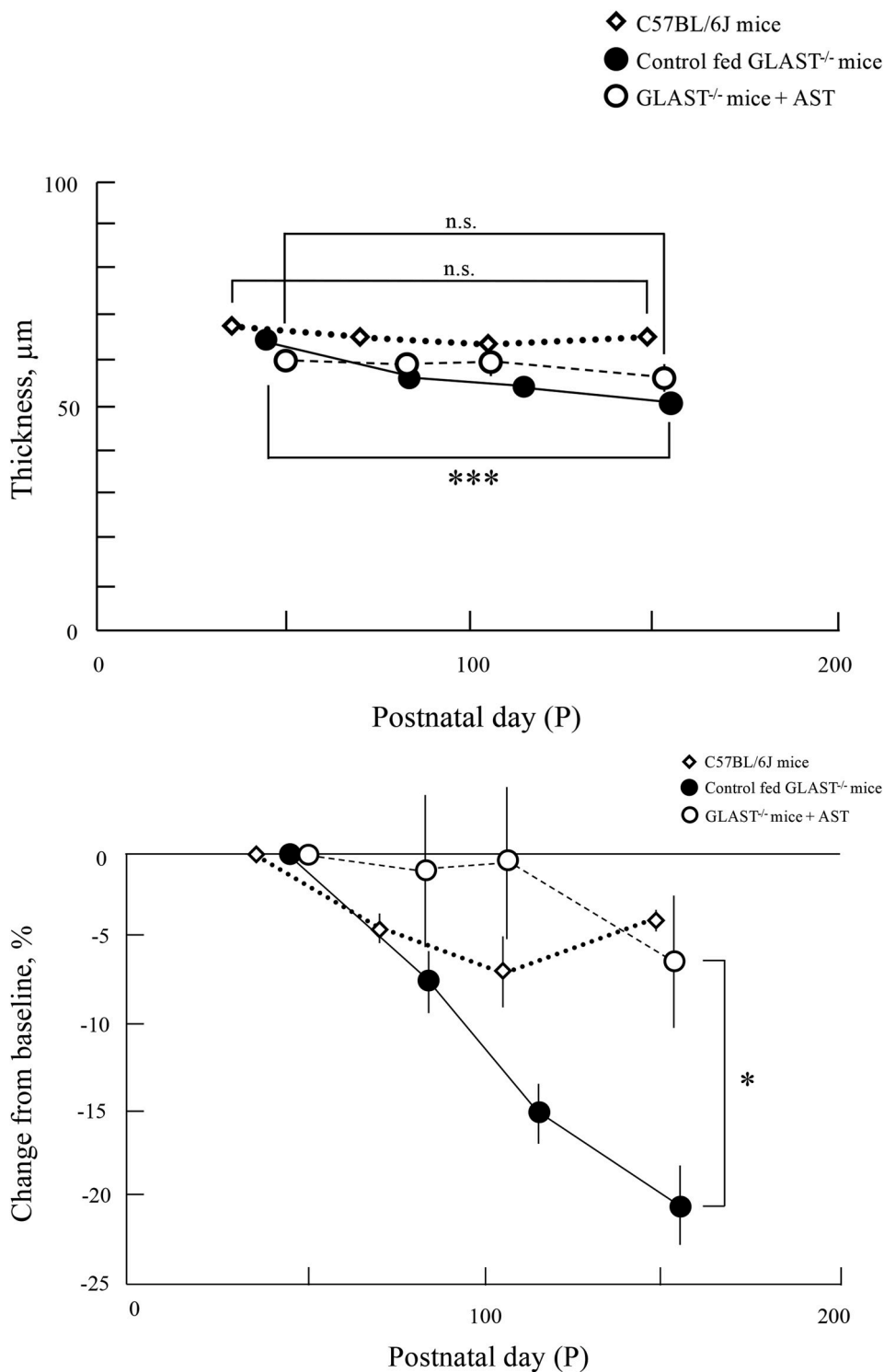
Fig. 2. (*continued*).

the GCC was calculated using raw data summarized in an Excel® file generated by the InSight® software program. The overall average GCC thickness was presented as the mean ± standard error.

2.4. Ultrastructural examination by electron microscopy

Electron microscopy was performed using eyes enucleated from GLAST$^{-/-}$ mice + AST on P131, control fed GLAST$^{-/-}$ mice on P127, and C57BL/6J mice on P147 according to a previously described method

Table 1

The thickness (μm) of the GCC in C57BL/6J mice, control fed GLAST-/- mice, and GLAST-/- mice + AST.

	point 1 (baseline)	point 2	point 3	point 4
C57BL6J mice	67.93 ± 1.35	64.74 ± 0.62 (95.30%)	63.04 ± 1.48 (92.80%)	65.15 ± 0.45 (95.91%)
Control fed GLAST-/- mice	63.90 ± 1.31	58.90 ± 1.22 (92.18%)	53.93 ± 1.18 (84.40%)	50.69 ± 1.52 (79.33%)
GLAST-/- mice + AST	59.74 ± 2.15	59.15 ± 2.42 (99.01%)	59.51 ± 2.78 (99.61%)	55.87 ± 2.79 (93.52%)

Values indicate the mean ± standard error. The numbers in parentheses indicate the percentage in comparison to baseline.

[26]. Immediately after enucleation, the eyes were fixed with 2.5% glutaraldehyde and 2% paraformaldehyde solution at pH 7.4 for 24 h at 4 °C. An aliquot of the same fixation solution was injected into the anterior chamber. The retina and choroid were dissected out, post-fixed in phosphate buffered 1% osmium tetroxide at pH 7.4 for 3 h at 4 °C, dehydrated in an ascending ethanol series (50–100%), and embedded in epoxy resin. Thin sections (80–90 nm) were stained in uranyl and lead salt solutions. The sections were photographed by a transmission electron microscope (H-7600, Hitachi, Tokyo, Japan) at 100 kV.

2.5. Statistical analysis

The statistical analysis of the data obtained in the present study was performed using the SPSS software program (version 26, Statistical Package for the Social Sciences, Chicago, IL, U.S.A.). The normality of the distribution of the segmentation data from the three groups was confirmed using the Shapiro-Wilk test. Parametric or non-parametric methods were chosen according to the presence of normality. Student's *t*-test was performed to analyze differences in the GCC thickness obtained by SD-OCT segmentation between the baseline and final observation points in each group (GLAST$^{-/-}$ mice + AST, P50 vs. P157; control fed GLAST$^{-/-}$ mice, P44 vs. P156; C57BL/6J mice, P36 vs. P148; respectively) (Fig. 2B). In addition, Student's *t*-test was performed to analyze differences in change from baseline to the final observation points in the GCC thickness obtained by SD-OCT segmentation between GLAST$^{-/-}$ mice + AST and control fed GLAST$^{-/-}$ mice. P values of <0.05 were considered to indicate statistical significance.

3. Results

3.1. Qualitative analyses of the ganglion cell complex obtained by SD-OCT

We analyzed the GCC on SD-OCT images of GLAST$^{-/-}$ mice + AST, control fed GLAST$^{-/-}$ mice, and C57BL/6J mice to qualitatively characterize the SD-OCT findings (Fig. 2A). Typical SD-OCT findings in C57BL/6J mice obtained from P36 to P148 are shown in Fig. 2A, a, b, c and d. Conversely, the SD-OCT findings in control fed GLAST$^{-/-}$ mice obtained from P44 to P156 are shown in Fig. 2A, e, f, g and h. And the SD-OCT findings in the GLAST$^{-/-}$ mice + AST obtained from P50 to P150 are shown in Fig. 2A, i, j, k and l. As previously reported, it was found that in control fed GLAST$^{-/-}$ mice the GCC became thinner due to the loss of RGCs and thinning of RNFL in comparison to both GLAST$^{-/-}$ mice + AST and C57BL/6J mice [9]. The SD-OCT findings at the final observation point are shown in Fig. 2B. The GCC thickness in both GLAST$^{-/-}$ mice + AST and C57BL/6J mice qualitatively appeared thicker than the control fed GLAST$^{-/-}$ mice. To confirm statistical significance, we longitudinally and quantitatively analyzed the GCC thickness obtained by SD-OCT in each group. The results in this study are shown in Fig. 2C and Table 1. The thickness of GCC in the control fed GLAST$^{-/-}$ mice between the baseline and final observation points are significantly changed, but not in other groups. Fig. 2D shows the change in the GCC thickness from the mean values at baseline to each observation point. The rate of reduction was significantly different between GLAST$^{-/-}$ mice + AST and control fed GLAST$^{-/-}$ mice.

3.2. The ultrastructural findings of the RNFL and RGCs in each group

The electron microscopic findings of each group are shown in Fig. 3. Panel a corresponds to the C57BL/6J mice at P147, Panel b corresponds to the control fed GLAST$^{-/-}$ mice at P131, and Panel c corresponds to the GLAST$^{-/-}$ mice + AST at P127, respectively. Arrows indicate the RNFL thickness in each panel. The RNFL thickness in control fed GLAST$^{-/-}$ mice were qualitatively thinner than the other groups, as shown in Fig. 3a–c.

4. Discussion

In the present study, we first showed that AST attenuates the thinning of the GCC in GLAST$^{-/-}$ mice. The rate of reduction of the GCC thickness in GLAST$^{-/-}$ mice + AST was almost similar to that of C57BL/6J mice. Furthermore, electron microscopy demonstrated that the RNFL thickness in GLAST$^{-/-}$ mice + AST and C57BL/6J mice were qualitatively thicker than the control fed GLAST$^{-/-}$ mice. The thicker RNFL indicates that AST suppressed the cell death of RGCs in GLAST$^{-/-}$ mice.

In the retina, GLAST is expressed in Müller cells and maintains

C57BL/6J mice, P147   Control fed GLAST$^{-/-}$ mice, P131   GLAST$^{-/-}$ mice + AST, P127

(a)   (b)   (c)
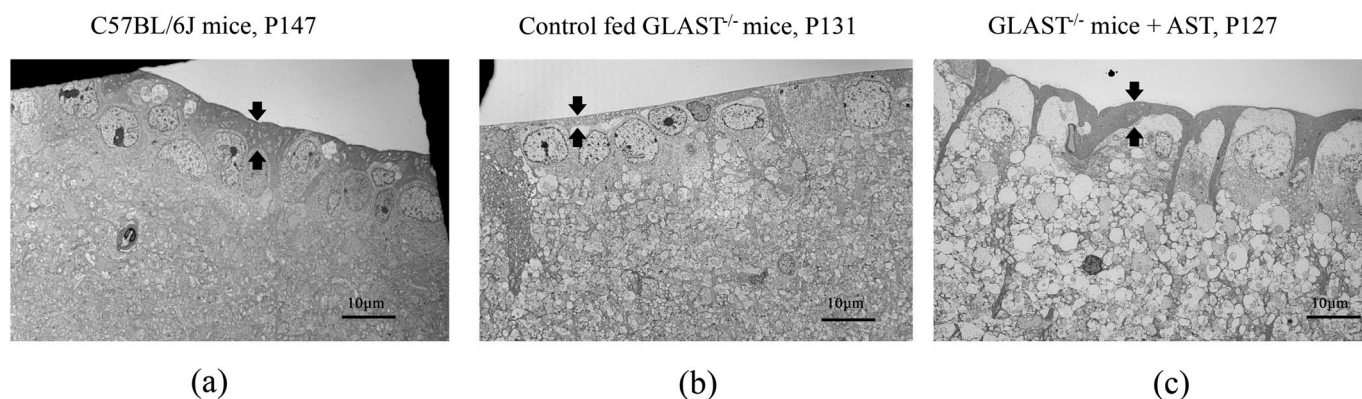
Fig. 3. Comparison of the retinal nerve fiber layer and ganglion cell layer observed by electron microscopy in C57BL/6J mice, control fed GLAST$^{-/-}$ mice, and GLAST$^{-/-}$ mice + AST. Panel a corresponds to C57BL/6J mice at P147. Panel b corresponds to control fed GLAST$^{-/-}$ mice at P131. Panel c corresponds to GLAST$^{-/-}$ mice + AST at P127. Arrows indicate the RNFL thickness in each panel.

glutamate homeostasis by taking up the extracellular glutamate released for glutamatergic neurotransmission into the Müller cells [10]. Moreover, GLAST is essential not only for keeping the extracellular glutamate concentration below the neurotoxic level, but also for maintaining the glutathione levels in the retina by providing the substrate for glutathione synthesis [9,11]. Thus, glutamate neurotoxicity and oxidative stress increase in the GLAST$^{-/-}$ mouse retina. The GLAST$^{-/-}$ mouse is used as a model of NTG because it shows similar morphological changes to glaucoma due to the loss of RGCs without an elevated IOP, and the loss of RGCs is thought to be caused by both glutamate neurotoxicity and oxidative stress [9]. Actually, both glutamate neurotoxicity and decreasing GSH are also considered an etiology of glaucoma [4,6]. Thus, GLAST$^{-/-}$ mice are used to elucidate the pathogenesis of NTG. Recently, several studies have reported that many agents, including geranylgeranylacetone, an acylic isoprenoid, VCP modulator, a major ATPase in the cell, dedicator of cytokinesis 3, a guanine nucleotide exchange factor and a novel NR2D interacting protein, and valproic acid used for treatment of epilepsy, mood disorders, migraines and neuropathic pain, protected the RGCs in GLAST heterozygous or deficient mice [27–30]. Moreover, it is thought that glutamate neurotoxicity may play a bigger role than oxidative stress in RGC death in GLAST$^{-/-}$ mice [21]. Thus, it may suggest that AST—rather than oxidative stress—reduced glutamate neurotoxicity in our study. This also means that AST may reduce glutamate neurotoxicity, as was reported in previous *in vitro* studies [16, 17].

AST is a natural marine carotenoid and can be used as a health supplement. Recently, AST was reported to possess a wide variety of biological functions. In particular, as a strong antioxidant, AST effectively scavenges oxygen free radicals and reduces oxidative stress [13]. AST also reduces oxidative stress in the retina [31]. In addition, in cultured neural cells, AST protects cells against glutamate-induced apoptosis [16,17]. For these reasons, we investigated whether or not AST has a protective effect in the GCC of GLAST$^{-/-}$ mice, because the RGC degeneration of GLAST$^{-/-}$ mice is caused by both glutamate neurotoxicity and oxidative stress. As expected, AST had a protective effect against thinning of the GCC in GLAST$^{-/-}$ mice.

In previous studies of mice fed with AST, the effect of AST was observed at concentrations of 0.03%–0.5% [32–34]. Among them, Yook et al. examined mice fed a diet containing AST (0, 0.02, 0.1, and 0.5%) for supplementation to define the effect of AST on adult hippocampal neurogenesis [32]. Their findings revealed that AST enhanced cell proliferation and survival at doses of 0.1% and 0.5%. Based on the results of these studies, in the present study, we used 0.1% AST so that nutritional status was maintained, even in the AST group.

The present study was associated with some limitations. First, although we hypothesized that AST attenuates the thinning of the GCC thickness via a reduction of oxidative stress and glutamate neurotoxicity, we did not measure the quantitative levels of some of the oxidative stress and cell death induced by glutamate neurotoxicity. However previous studies have shown that AST reduces oxidative stress in the retina, in addition, AST was shown to attenuate glutamate-induced apoptosis and cytotoxicity in *in vitro* studies [16,17]. Thus, it suggests that oxidative stress and glutamate-induced apoptosis and cytotoxicity may be decreased in our study. Second, it is unclear whether AST was more effective for glutamate neurotoxicity or oxidative stress to attenuate the thinning of the GCC in GLAST$^{-/-}$ mice. Third, although it has been reported that GLAST$^{-/-}$ mice showed impaired retinal function examined by multifocal electroretinogram [9], we did not analyze the retinal functions but mainly focused on the morphological changes evaluated by SD-OCT in this study. Since several studies have reported that the thinning of the RGCs layer ameliorated retinal function in GLAST$^{-/-}$ mice by interventional studies [23,31], it can be expected that AST treatment prevents the decline in retinal function of GLAST$^{-/-}$ mice. Fourth, although we did not investigate molecular mechanisms of effects of AST in GLAST$^{-/-}$ mice, it needs to be further clarified in the future study.

In conclusion, we found that AST attenuates the thinning of the GCC in GLAST$^{-/-}$ mice. Our results suggest the possibility that AST has protective effects against glutamate neurotoxicity and oxidative stress *in vivo*. Because reducing IOP as much as possible is the only currently available treatment for NTG in the clinical setting, our results suggest that AST supplementation may be effective for protecting against some factors involved in NTG, such as glutamate neurotoxicity and oxidative stress.

Author statement

In this study, we have first clarified that astaxanthin may protect retinal ganglion cell loss happened in GLAST knock-out mice, a mouse model of normal tension glaucoma.

We declare that the contents of this manuscript have neither been published nor been under consideration for publication in any journals.

Declaration of competing interest

There is no conflict of interest regarding the study described in the manuscript.

Acknowledgements

References

[1] A.S. Mursch-Edlmayr, N. Luft, D. Podkowinski, M. Ring, L. Schmetterer, M. Bolz, Laser speckle flowgraphy derived characteristics of optic nerve head perfusion in normal tension glaucoma and healthy individuals: a Pilot study, Sci. Rep. 8 (2018) 5343.

[2] A. Meguro, H. Inoko, M. Ota, N. Mizuki, S. Bahram, Genome-wide association study of normal tension glaucoma: common variants in SRBD1 and ELOVL5 contribute to disease susceptibility, Ophthalmology 117 (2010) 1331–1338.

[3] X.S. Mi, T.F. Yuan, K.F. So, The current research status of normal tension glaucoma, Clin. Interv. Aging 9 (2014) 1563–1571.

[4] D. Gherghel, S. Mroczkowska, L. Qin, Reduction in blood glutathione levels occurs similarly in patients with primary-open angle or normal tension glaucoma, Invest. Opthalmol. Vis. Sci. 54 (2013) 3333–3339.

[5] A. Kimura, K. Namekata, X. Guo, T. Noro, C. Harada, T. Harada, Targeting oxidative stress for treatment of glaucoma and optic neuritis, Oxid. Med. Cell. Longev. 2017 (2017) 1–8.

[6] K. Evangelho, M. Mogilevskaya, M. Losada-Barragan, J.K. Vargas-Sanchez, Pathophysiology of primary open-angle glaucoma from a neuroinflammatory and neurotoxicity perspective: a review of the literature, Int. Ophthalmol. 39 (2019) 259–271.

[7] H.W. Bae, S.J. Seo, S.Y. Lee, Y.H. Lee, G.J. Seong, C.Y. Kim, Risk factors for visual field progression of normal-tension glaucoma in patients with myopia, Can. J. Ophthalmol. 52 (2017) 107–113.

[8] V. Gupta, Y. You, J. Li, V. Gupta, M. Golzan, A. Klistorner, M. van den Buuse, S. Graham, BDNF impairment is associated with age-related changes in the inner retina and exacerbates experimental glaucoma, Biochim. Biophys. Acta 1842 (2014) 1567–1578.

[9] T. Harada, C. Harada, K. Nakamura, H.M. Quah, A. Okumura, K. Namekata, T. Saeki, M. Aihara, H. Yoshida, A. Mitani, K. Tanaka, The potential role of glutamate transporters in the pathogenesis of normal tension glaucoma, J. Clin. Invest. 117 (2007) 1763–1770.

[10] T. Rauen, M. Wiessner, Fine tuning of glutamate uptake and degradation in glial cells: common transcriptional regulation of GLAST1 and GS, Neurochem. Int. 37 (2000) 179–189.

[11] W. Reichelt, J. Stabel-Burow, T. Pannicke, H. Weichert, U. Heinemann, The glutathione level of retinal Müller glial cells is dependent on the high-affinity sodium-dependent uptake of glutamate, Neuroscience 77 (1997) 1213–1224.

[12] D. Huster, A. Reichenbach, W. Reichelt, The glutathione content of retinal Müller (glial) cells: effect of pathological conditions, Neurochem. Int. 36 (2000) 461–469.

[13] C. Galasso, I. Orefice, P. Pellone, P. Cirino, R. Miele, A. Ianora, C. Brunet, C. Sansone, On the neuroprotective role of astaxanthin: new perspectives? Mar. Drugs 16 (2018) 247.

[14] P. Nagendraprabhu, G. Sudhandiran, Astaxanthin inhibits tumor invasion by decreasing extracellular matrix production and induces apoptosis in experimental

rat colon carcinogenesis by modulating the expressions of ERK-2, NFkB and COX-2, Invest. N. Drugs 29 (2011) 207–224.

[15] N.S. Mashhadi, J. Zakerkish, J. Mohammadiasl, M. Zarei, M. Mohammadshahi, M. H. Haghighizadeh, Astaxanthin improves glucose metabolism and reduces blood pressure in patients with type 2 diabetes mellitus, Asia Pac, J. Clin. Nutr. 27 (2018) 341–346.

[16] X. Wen, A. Huang, J. Hu, Z. Zhong, Y. Liu, Z. Li, X. Pan, Z. Liu, Neuroprotective effect of astaxanthin against glutamate-induced cytotoxicity in HT22 cells: involvement of the Akt/GSK-3β pathway, Neuroscience 303 (2015) 558–568.

[17] X. Lin, Y. Zhao, S. Li, Astaxanthin attenuates glutamate-induced apoptosis via inhibition of calcium influx and endoplasmic reticulum stress, Eur. J. Pharmacol. 806 (2017) 43–51.

[18] T. Otsuka, M. Shimazawa, T. Nakanishi, Y. Ohno, Y. Inoue, K. Tsuruma, T. Ishibashi, H. Hara, The protective effects of a dietary carotenoid, astaxanthin, against light-induced retinal damage, J. Pharmacol. Sci. 123 (2013) 209–218.

[19] K. Izumi-Nagai, N. Nagai, K. Ohgami, S. Satufuka, Y. Ozawa, K. Tsubota, S. Ohno, Y. Oike, S. Ishida, Inhibition of choroidal neovascularization with an anti-inflammatory carotenoid astaxanthin, Invest. Ophthalmol. Vis. Sci. 49 (2008) 1679–1685.

[20] A. Küçüködük, F. Helvacioglu, N. Haberal, A. Dagdeviren, D. Bacanli, G. Yilmaz, I. Akkoyun, Antiproliferative and anti-apoptotic effect of astaxanthin in an oxygen-induced retinopathy mouse model, Can. J. Ophthalmol. 54 (2019) 65–74.

[21] H. Sano, K. Namekata, A. Kimura, H. Shitara, X. Guo, C. Harada, Y. Mitamura, T. Harada, Differential effects of N-acetylcysteine on retinal degeneration in two mouse models of normal tension glaucoma, Cell Death Dis. 10 (2019) 75.

[22] S. Schneider, W. Mellert, S. Schulte, B. van Ravenzwaay, A developmental toxicity study of 3S, 3'S-Astaxanthin in New Zealand white rabbits, Food Chem. Toxicol. 90 (2016) 95–101.

[23] M.A. Zielińska, A. Wesołowska, B. Pawlus, J. Hamułka, Health effects of carotenoids during pregnancy and lactation, Nutrients 9 (2017) 838.

[24] T. Gonome, Y. Xie, S. Arai, K. Yamauchi, N. Maeda-Monai, R. Tanabu, T. Kudo, M. Nakazawa, Excess glutamate may cause dilation of retinal blood vessels in glutamate/aspartate transporter-deficient mice, BioMed Res. Int. 2019 (2019) 1–11.

[25] R. Tanabu, K. Sato, N. Monai, K. Yamauchi, T. Gonome, Y. Xie, S. Takahashi, S.-I. Ishiguro, M. Nakazawa, The findings of optical coherence tomography of retinal degeneration in relation to the morphological and electroretinographic features in RPE65$^{-/-}$ mice, PLoS One 14 (2019), e0210439.

[26] K. Yamauchi, R. Tanabu, N. Monai, T. Gonome, Y. Xie, S. Takahashi, S.-I. Ishiguro, M. Nakazawa, The spectral-domain optical coherence tomography findings associated with the morphological and electrophysiological changes in a rat model of retinal degeneration, rhodopsin S334ter-4 rats, BioMed Res. Int. 2018 (2018) 1–10.

[27] Z. Dong, Y. Shinmei, Y. Dong, S. Inafuku, J. Fukuhara, R. Ando, N. Kitaichi, A. Kanda, K. Tanaka, K. Noda, T. Harada, S. Chin, S. Ishida, Effect of geranylgeranylacetone on the protection of retinal ganglion cells in a mouse model of normal tension glaucoma, Heliyon 2 (2016), e00191.

[28] N. Nakano, H. Ikeda-Ohashi, T. Hasegawa, Y. Muraoka, S. Iwai, T. Tsuruyama, M. Nakano, T. Fuchigami, T. Shudo, A. Kakizuka, N. Yoshimura, Neuroprotective effects of VCP modulators in mouse models of glaucoma, Heliyon 2 (2016), e00096.

[29] N. Bai, H. Hayashi, T. Aida, K. Namekata, T. Harada, M. Mishina, K. Tanaka, Dock3 interaction with a glutamate-receptor NR2D subunit protects neurons from excitotoxicity, Mol. Brain 6 (2013) 1–11.

[30] A. Kimura, X. Guo, T. Noro, C. Harada, K. Tanaka, K. Namekata, T. Harada, Valproic acid prevents retinal degeneration in a murine model of normal tension glaucoma, Neurosci. Lett. 588 (2014) 108–113.

[31] P.T. Yeh, H.W. Huang, C.M. Yang, W.S. Yang, C.H. Yang, Astaxanthin inhibits expression of retinal oxidative stress and inflammatory mediators in streptozotocin-induced diabetic rats, PLoS One 11 (2016), e0146438.

[32] J.S. Yook, M. Okamoto, R. Rakwal, J. Shibato, M.C. Lee, T. Matsui, H. Chang, J. Y. Cho, H. Soya, Astaxanthin supplementation enhances adult hippocampal neurogenesis and spatial memory in mice, Mol. Nutr. Food Res. 60 (2016) 589–599.

[33] R. Nakao, O.L. Nelson, J.S. Park, B.D. Mathison, P.A. Thompson, B.P. Chew, Effect of astaxanthin supplementation on inflammation and cardiac function in BALB/c mice, Anticancer Res. 30 (2010) 2721–2725.

[34] Y. Yang, T.X. Pham, C.J. Wegner, B. Kim, C.S. Ku, Y.K. Park, J.Y. Lee, Astaxanthin lowers plasma TAG concentrations and increases hepatic antioxidant gene expression in diet-induced obesity mice, Br. J. Nutr. 112 (2014) 1797–1804.